

## Supporting Information

### Synergistically enhanced oxygen reduction activity of MnO<sub>x</sub>- CeO<sub>2</sub>/ketjenblack composite

Jiajie Chen,<sup>a</sup> Nan Zhou,<sup>b</sup> Haiyan Wang,<sup>a,c,\*</sup> Zhiguang Peng,<sup>a</sup> Huiyong Li,<sup>b</sup> Yougen Tang<sup>a,\*</sup> and Kun

Liu<sup>a</sup>

<sup>a</sup> College of Chemistry and Chemical Engineering, Central South University, Changsha, 410083, P.R. China.

E-mail: [wanghy419@126.com](mailto:wanghy419@126.com); [ygtang@csu.edu.cn](mailto:ygtang@csu.edu.cn). Tel.: +86 0731 8830886; fax: +86 0731 8879616.

<sup>b</sup> College of Science, Hunan Agricultural University, Changsha, 410128, P.R. China.

<sup>c</sup> State Key Laboratory for Powder Metallurgy, Central South University, Changsha 410083, China

## Experimental Section

### 1. Synthesis of CeO<sub>2</sub>/KB, MnO<sub>x</sub>/KB and MnO<sub>x</sub>-CeO<sub>2</sub>/KB

Carbon support KB (ketjenblack carbon, EC-300J) was treated in HNO<sub>3</sub> at 80 °C for 8 h to remove metal impurities and introduce oxygen containing functional groups on the carbon surface. After that, KB was washed with distilled water at least 10 times and then dried in air at 110 °C. CeO<sub>2</sub>/KB was prepared by a simple hydrothermal method. Briefly, 1.094 g Ce(NO<sub>3</sub>)<sub>3</sub>·6H<sub>2</sub>O was first dissolved into 70 ml distilled water to prepare aqueous Ce(NO<sub>3</sub>)<sub>3</sub> solution, then 1g acid-treated KB was added into the Ce(NO<sub>3</sub>)<sub>3</sub> solution. This suspension was stirred for at least 30 min before being transferred into a 100 mL Teflon-lined autoclave and then kept at 160 °C for 8 h. The prepared CeO<sub>2</sub>/KB was filtered and dried in air at 110 °C. For MnO<sub>x</sub>-CeO<sub>2</sub>/KB, 0.1 g CeO<sub>2</sub>/KB was added into 20 mL distilled water with continuous stirring. Then 25 mL KMnO<sub>4</sub> solution (0.2 wt%) was slowly added into the suspension prepared before. After the mixture was kept at 70 °C for 1 h, the suspension was filtered, washed, and dried at 110 °C. For comparison, the MnO<sub>x</sub>/KB catalyst was also prepared through the similar procedure as MnO<sub>x</sub>-CeO<sub>2</sub>/KB using 0.0854 g acid-treated KB instead of 0.1 g CeO<sub>2</sub>/KB. All as-prepared samples were heated at 400 °C for 2 h

under flowing Ar.

## 2. Materials Characterization

X-ray diffraction (XRD) patterns of as-prepared samples were recorded by X-ray diffractometer (Dandong Haoyuan, DX-2700) utilizing a Cu-K $\alpha$ 1 source with a step of 0.02°. Scanning electron microscope (SEM) images of as-prepared MnO<sub>x</sub>-CeO<sub>2</sub>/KB were conducted using a Nova NanoSEM 230 SEM. Transmission electron microscope (TEM), high resolution TEM (HRTEM) images, scanning TEM (STEM) and elemental mapping of as-prepared MnO<sub>x</sub>-CeO<sub>2</sub>/KB were obtained using a FEI Tecnai G2 F20 S-TWIX TEM. Thermogravimetric analysis (TGA) was performed on a STA 449C with a heating rate of 10 °C/min from 25 to 800 °C. The XPS fitting was performed using XPSPEAK software. The specific surface area was calculated by using the BET equation from the N<sub>2</sub> adsorption isotherm.

## 3. Rotating disk electrode (RDE) measurements.

For the RDE measurements, 2 mg catalyst was dissolved in a 1 mL solvent mixture of 50 uL Nafion (5 wt %) and 950 uL ethanol by at least 40 min sonication to form a homogeneous ink. Then 10 uL of the catalyst ink was loaded onto on a glassy carbon rotating disk electrode of 5.61 mm in diameter (Pine Instrument Company, USA), which yielded a loading of catalyst 80.9 ug cm<sup>-2</sup>. 0.1 M KOH was used as an electrolyte, pure oxygen gas (99.999%) was purged for at least 20 min before each RDE experiment to make the electrolyte saturated with oxygen. Pt wire and saturated calomel electrode (SCE) were used as a counter and reference electrodes, respectively. All potentials initially measured verse the SCE were calibrated with respect to reversible hydrogen electrode (RHE).<sup>1</sup> The working electrode was scanned cathodically at a rate of 10 mV s<sup>-1</sup> with varying rotating speed from 400 rpm to 1600 rpm. Koutecky-Levich plots were analyzed at various electrode potentials. The slopes of their linear fit lines are used to calculate the electron transfer number ( $n$ ) on the basis of the Koutecky-Levich equation:<sup>2</sup>

$$\frac{1}{j} = \frac{1}{j_L} + \frac{1}{j_K} = \frac{1}{B\omega^{1/2}} + \frac{1}{j_K}$$

$$B = 0.62nFC_0D_0^{2/3}\nu^{-1/6}$$

For the Tafel plot, the kinetic current was calculated as follows:

$$j_K = \frac{j \times j_L}{j_L - j}$$

Where  $j$  is the experimentally measured current density,  $j_L$  is the diffusion-limiting current density,  $j_K$  is the kinetic current density,  $\omega$  is the electrode rotating speed in rpm,  $F$  is the Faraday constant,  $C_0$  is the bulk concentration of  $O_2$ ,  $D_0$  is the diffusion coefficient of  $O_2$ , and  $\nu$  is the kinematic viscosity of the electrolyte. The kinetic mass activity ( $j_m$ ) was calculated via the normalization of the kinetic current ( $j_K$ ) with the catalyst mass loading.

## Supporting Figures

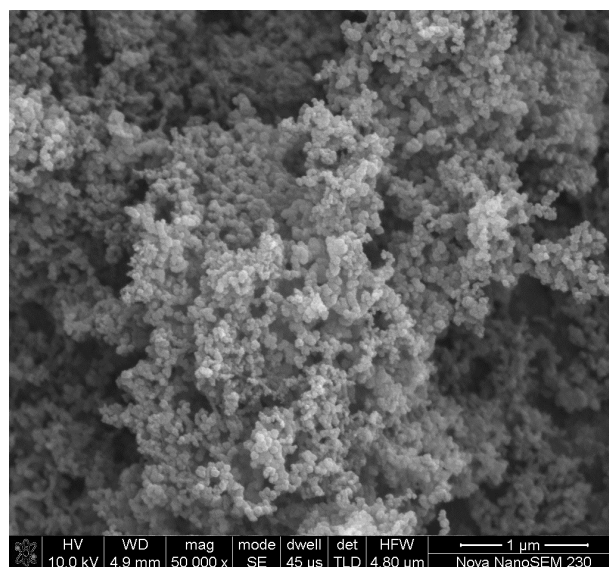


**Fig. S1** Typical SEM image of  $MnO_x$ - $CeO_2$ /KB hybrid.

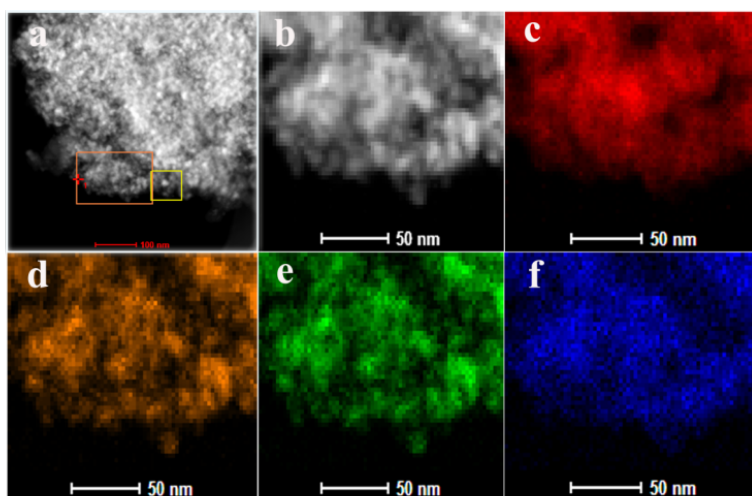


**Fig. S2** STEM and elemental mapping analysis of the  $\text{MnO}_x\text{-CeO}_2/\text{KB}$  hybrid. (a) Typical STEM image. (b) STEM image taken from the left selected region marked in (a). (c-f) Corresponding elemental mapping images of (c) C, (d) O, (e) Mn, and (f) Ce.

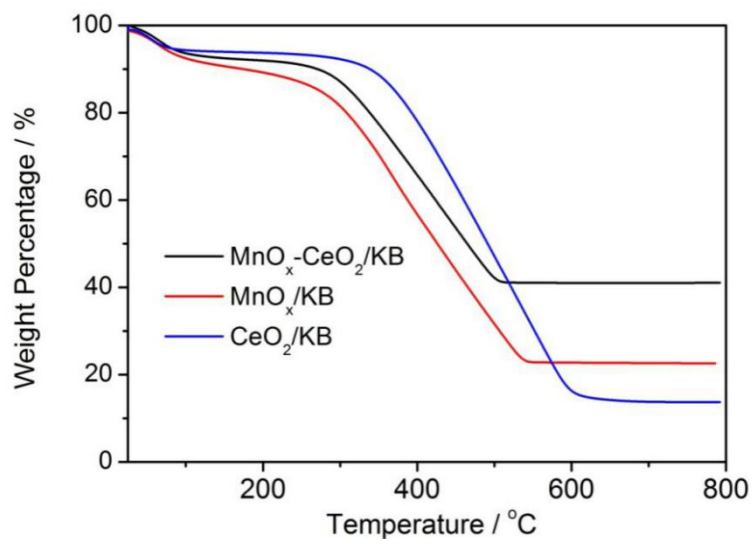


**Fig. S3** TGA curves of  $\text{MnO}_x\text{-CeO}_2/\text{KB}$ ,  $\text{MnO}_x/\text{KB}$  and  $\text{CeO}_2/\text{KB}$  in air.

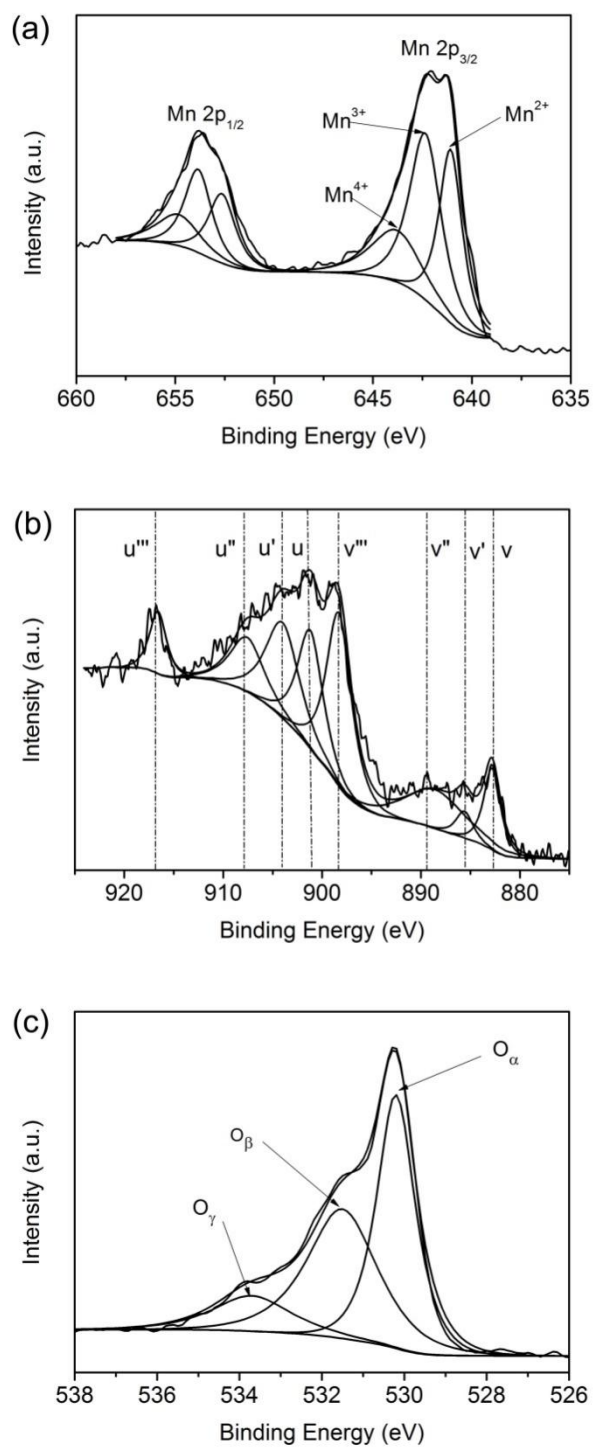


**Fig. S4** XPS spectra of Mn 2p (a), Ce 3d (b) and O 1s (c) in the MnO<sub>x</sub>-CeO<sub>2</sub>/KB hybrid.

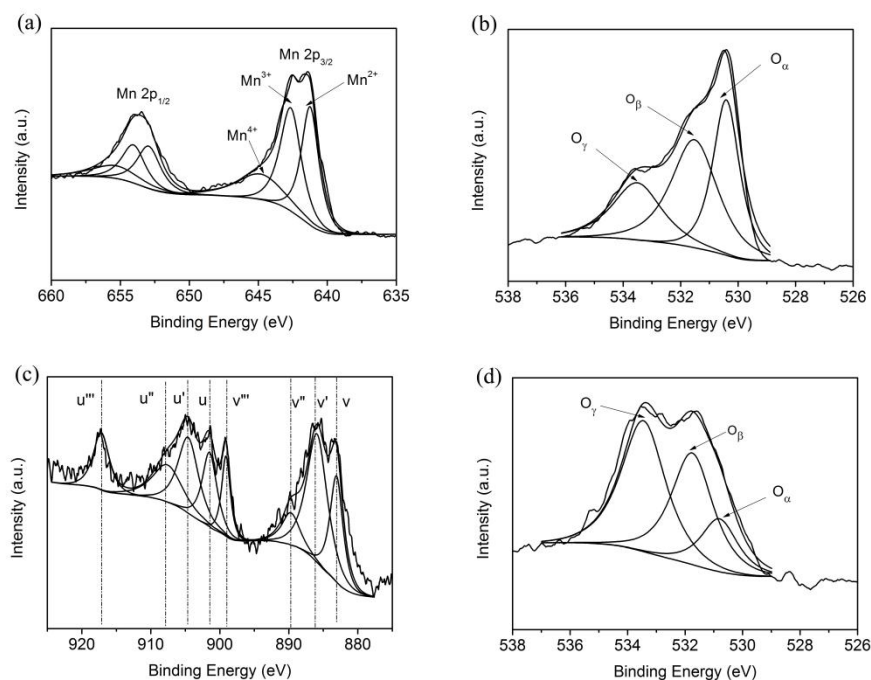


**Fig. S5** XPS spectra of Mn 2p (a), O 1s (b) in  $\text{MnO}_x/\text{KB}$  and Ce 3d (c), O 1s (d) in  $\text{CeO}_2/\text{KB}$ .

The Mn 2p and O 1s spectra in  $\text{MnO}_x/\text{KB}$  are similar to those of the  $\text{MnO}_x\text{-CeO}_2/\text{KB}$  hybrid. The Ce 3d (c), O 1s (d) in  $\text{CeO}_2/\text{KB}$  are a little different with those of  $\text{MnO}_x\text{-CeO}_2/\text{KB}$  hybrid. The peak marked as v' in  $\text{CeO}_2/\text{KB}$  is much stronger than that in  $\text{MnO}_x\text{-CeO}_2/\text{KB}$ , indicating that the proportion of  $\text{Ce}^{3+}$  species in  $\text{CeO}_2/\text{KB}$  is larger than that of  $\text{MnO}_x\text{-CeO}_2/\text{KB}$ , which is associated with a larger proportion of defect oxygen ( $\text{O}_\beta/\text{O}_\alpha+\text{O}_\beta$ ). The decrease of  $\text{Ce}^{3+}$  species and defect oxygen in  $\text{MnO}_x\text{-CeO}_2/\text{KB}$  compared with  $\text{CeO}_2/\text{KB}$  may be due to the fact that the  $\text{MnO}_x$  nanoparticles are located in the vicinity of  $\text{CeO}_2$ . We can also conclude that the oxygen-containing functional groups decrease when  $\text{MnO}_x$  deposited on the carbon surface of  $\text{CeO}_2/\text{KB}$  since the peak denoted as  $\text{O}_\gamma$  in  $\text{MnO}_x\text{-CeO}_2/\text{KB}$  is much weaker than that in  $\text{CeO}_2/\text{KB}$ .

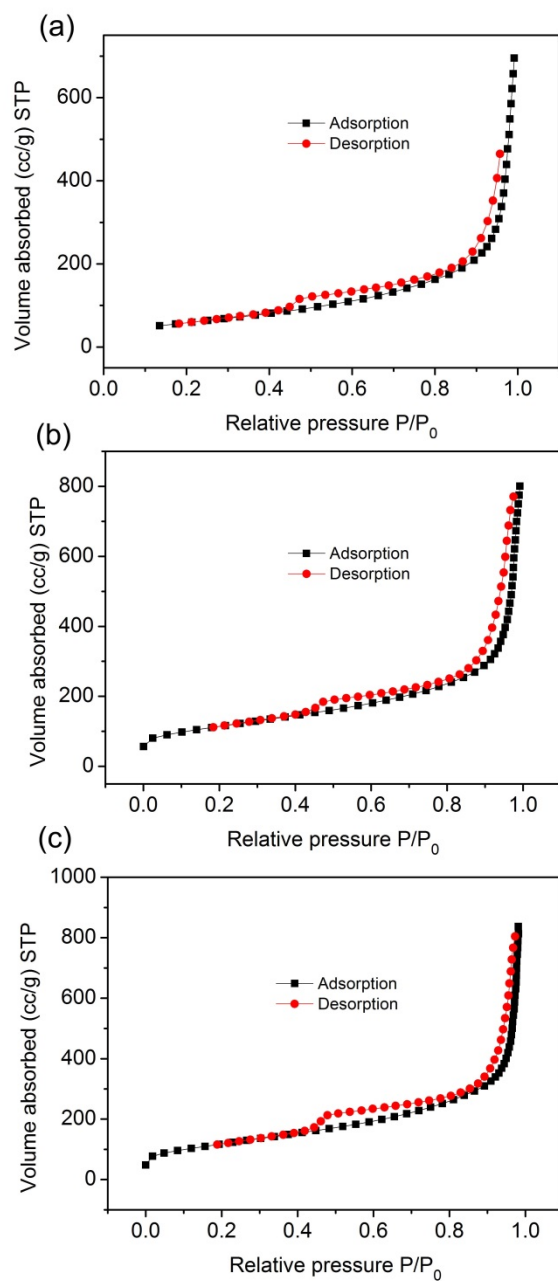


**Fig. S6**  $\text{N}_2$  adsorption-desorption isotherms of  $\text{MnO}_x\text{-CeO}_2/\text{KB}$  (a),  $\text{MnO}_x/\text{KB}$  (b) and  $\text{CeO}_2/\text{KB}$

(c).

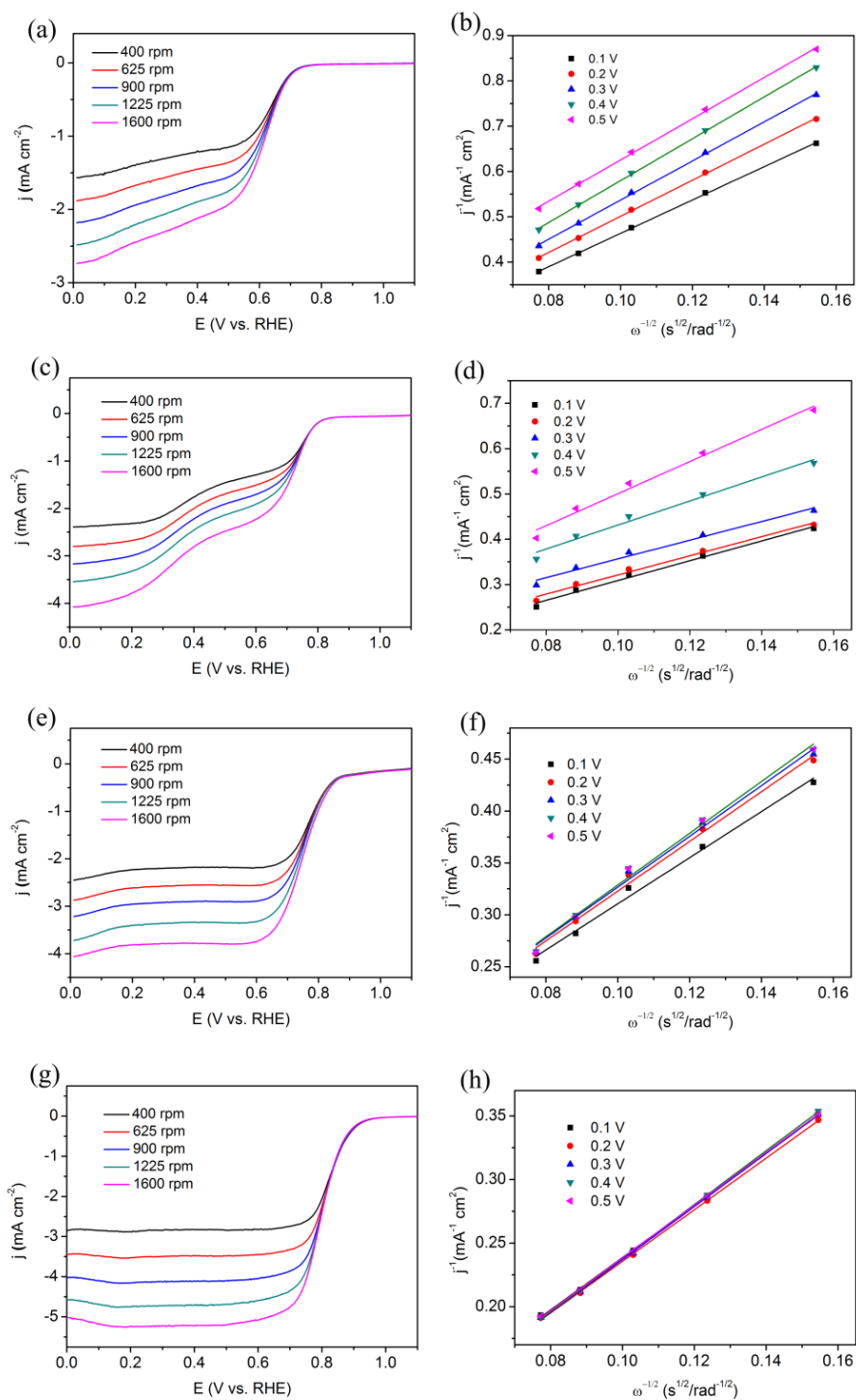


**Fig. S7** (a, c, e and g) Detailed LSV curves of KB, CeO<sub>2</sub>/KB, MnO<sub>x</sub>/KB and Pt/C at different rotating speeds using RDE in O<sub>2</sub> saturated 0.1 M KOH solution with a sweep rate of 10 mV s<sup>-1</sup>. Catalyst loading was 80.9 ug cm<sup>-2</sup> for all samples; (b, d, f and h) the calculated Koutecky-Levich plots for KB, CeO<sub>2</sub>/KB, MnO<sub>x</sub>/KB and Pt/C at different potentials.



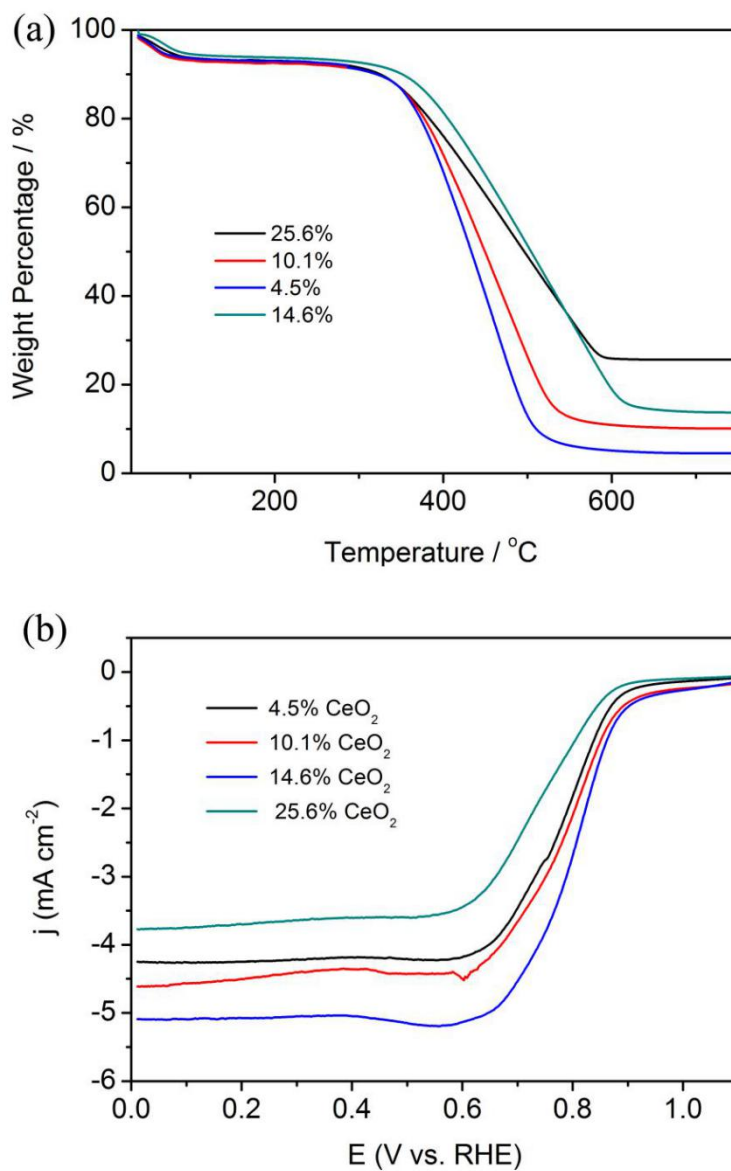


**Fig. S8** (a) TGA curves of different mass loading of CeO<sub>2</sub>/KB. (b) LSV curves of different mass loading of CeO<sub>2</sub> of MnO<sub>x</sub>-CeO<sub>2</sub>/KB using RDE in O<sub>2</sub> saturated 0.1 M KOH solution with a sweep rate of 10 mV s<sup>-1</sup>.

#### References:

1. Y. Meng, W. Song, H. Huang, Z. Ren, S.-Y. Chen and S. L. Suib, *Journal of the American Chemical Society*, 2014, **136**, 11452-11464.

2. H. Zhang, H. Li, H. Wang, K. He, S. Wang, Y. Tang and J. Chen, *Journal of Power Sources*, 2015, **280**, 640-648.